

Internal Quantum Efficiency and Carrier Injection Efficiency of c-plane, $\{10\bar{1}1\}$ and $\{11\bar{2}2\}$ InGaN/GaN-Based Light Emitting Diodes

Junjun Wang

The electroluminescence (EL) output power of c-plane light emitting diodes (LEDs) is much higher than that of semipolar $\{10\bar{1}1\}$ and $\{11\bar{2}2\}$ LEDs on sapphire at the same operation current. In order to elucidate the reasons for this behavior, we have fitted the pulsed EL data by the well-known ABC model to extract the internal quantum efficiency (IQE) and the carrier injection efficiency (CIE) to clarify which parameter weighs more for the poor EL output power of the semipolar LEDs. On our semipolar LEDs, we observe a CIE of only about 4%, whereas their c-plane counterparts show a CIE of nearly 80%. The IQE values are fairly the same for all three structures. The fit of resonant photoluminescence (PL) data at room temperature confirms the similar IQE values for all three structures.

1. Introduction

Nowadays, InGaN/GaN based light emitting diodes (LEDs) are widely used as visible light sources ranging from blue to green. Owing to the polar character of the nitride semiconductors, the strain in InGaN/GaN quantum wells (QWs) leads to an internal electric field resulting in a local separation of electrons and holes, reducing their recombination probability and hence decreasing the InGaN/GaN QW efficiency. Consequently, many groups are making efforts to fabricate semipolar/nonpolar InGaN/GaN based LEDs following different approaches [1, 2]. Nevertheless, the luminescence efficiency of semipolar/nonpolar LEDs on foreign substrates is typically inferior as compared to that of the c-plane ones regardless of the expected higher QW efficiency. Is the lower luminescence efficiency caused by actually lower QW efficiency or worse charge carrier transport into the QWs? In this study, we try to answer this question by separating the internal quantum efficiency (IQE) and the carrier injection efficiency (CIE) through fitting of the electroluminescence (EL) data with the well-known ABC model [3] for c-plane, $\{10\bar{1}1\}$ and $\{11\bar{2}2\}$ LEDs. The IQE was additionally determined via the fit of the photoluminescence (PL) data of the same structures in order to check the reliability of the EL fit.

2. Experimental

Epitaxial growth of all three LED structures was carried out in a low pressure MOVPE horizontal reactor AIX-200/4 RF-S using TMGa, TEGa, TMIIn, Cp₂Mg, SiH₄ and NH₃

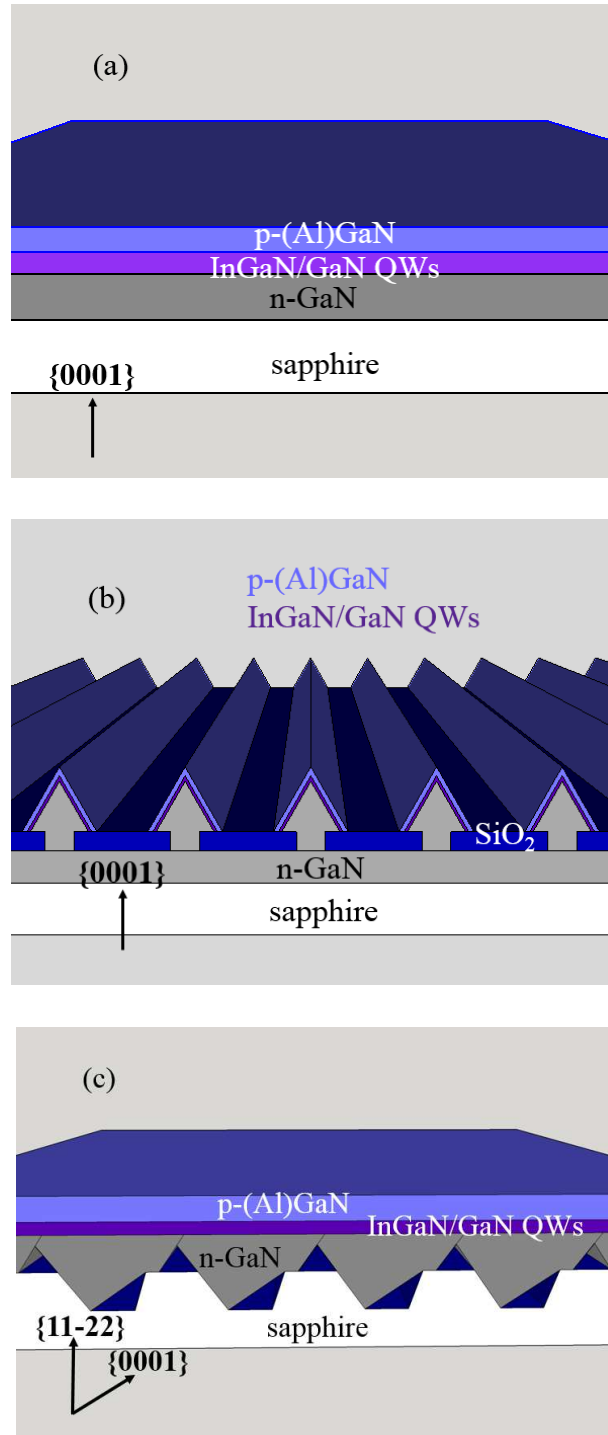


Fig. 1: Schematic structures of the c-plane (a), stripe $\{10\bar{1}1\}$ (b) and planar $\{11\bar{2}2\}$ (c) LEDs.

Table 1: The assumed values of the LEE and the calculated values of the CIE based on the fit for the c -plane LED, the stripe $\{10\bar{1}1\}$ LED and the planar $\{11\bar{2}2\}$ LED.

	LEE	CIE
c -plane LED	23 %	78 %
stripe $\{10\bar{1}1\}$ LED	40 %	4 %
planar $\{11\bar{2}2\}$ LED	40 %	4 %

as precursors. The c -plane LED was grown on a c -plane sapphire wafer consisting of $3\ \mu\text{m}$ thick n -GaN employing an in-situ deposited SiN nanomask layer for defect density reduction [4], 5-fold InGaN/GaN QWs as the active region with an InGaN thickness of 2.2 nm, 200 nm thick p -GaN capped with an excessively p -doped contact layer (Fig. 1a). To fabricate the $\{10\bar{1}1\}$ LED [5], firstly, a $3\ \mu\text{m}$ thick high quality n -doped GaN layer was grown on c -plane sapphire. Then, a 200 nm thick SiO_2 layer was deposited on the GaN template by plasma enhanced chemical vapor deposition (PECVD) and patterned into periodic stripes with $10\ \mu\text{m}$ wide masked area and $3\ \mu\text{m}$ wide opening along the $\langle 11\bar{2}0 \rangle$ crystal direction via photolithography and dry etching. Finally, 3D n -doped GaN stripes with triangular cross-section and a height of about $8.5\ \mu\text{m}$ were formed providing the $\{10\bar{1}1\}$ facet for the deposition of a single InGaN/GaN QW with the InGaN thickness of 2.5 nm and the subsequent layers to form the complete LED structure (Fig. 1b). A $\{10\bar{1}2\}$ sapphire was employed as the substrate for the $\{11\bar{2}2\}$ LED [6–8]. Firstly, the photoresist on the sapphire substrate is patterned into parallel stripes running along the sapphire a -direction with a period of $6\ \mu\text{m}$ via lithography. The stripe pattern is transferred into the sapphire substrate via reactive ion etching to achieve trenches with c -plane-like sidewalls. Then, SiO_2 is sputtered on top of all non c -plane-like facets to avoid parasitic GaN growth. Finally, the n -GaN growth starts from the c -plane-like sidewall and coalesces into a planar surface, the $\{11\bar{2}2\}$ facet, followed by 5-fold InGaN/GaN QWs with the InGaN thickness of 4.1 nm and p -(Al)GaN layers to complete the LED structure (Fig. 1c).

The LED structures are annealed at $750\ ^\circ\text{C}$ for 1 min in air for p -doping activation. On-wafer pulsed EL was applied with a pulse width of $1\ \mu\text{s}$ and a duty cycle of 1 % to avoid diode heating at large current densities. The external quantum efficiency (EQE) as an input data for the EL fit besides the measured current density j is evaluated from the experimental data according to the following equation:

$$\text{EQE} = \frac{\Phi q}{E_{\text{ph}} I} \quad \text{where} \quad E_{\text{ph}} = \frac{hc}{\lambda} \quad (1)$$

with E_{ph} representing the photon energy, Φ the radiant flux out of the LED, I the current flowing through the LED, q the elementary charge, h Planck's constant, c the speed of light in vacuum and λ the emission wavelength. The radiant flux Φ is measured in an integration sphere whereas the emission wavelength λ is obtained by a spectrometer. For the PL measurements, we employed a 405 nm laser diode as the excitation source to excite the carriers resonantly only in the QWs.

3. Fitting

According to the well-known ABC model, there are three recombination mechanisms, non-radiative Shockley-Read-Hall (SRH) recombination, radiative recombination and Auger recombination whose recombination rates are proportional to n , n^2 and n^3 , respectively, with n representing the carrier concentration. Then, the IQE can be expressed as

$$\text{IQE} = \frac{Bn^2}{An + Bn^2 + Cn^3}, \quad (2)$$

where A , B and C are the recombination rate coefficients.

In the case of EL, the external quantum efficiency (EQE) can be separated into three parts, CIE, IQE and light extraction efficiency (LEE):

$$\text{EQE} = \text{CIE} \cdot \text{LEE} \cdot \text{IQE}. \quad (3)$$

By inserting (2) into (3), the relation between EQE and the carrier concentration n can be written as

$$\text{EQE} = \text{CIE} \cdot \text{LEE} \cdot \frac{Bn^2}{An + Bn^2 + Cn^3}. \quad (4)$$

In steady state, the recombination rate R is equal to the carrier injection rate G_{inj} , $R = G_{\text{inj}}$.

$$R = An + Bn^2 + Cn^3, \quad (5)$$

$$G_{\text{inj}} = \frac{\text{CIE} \cdot I}{qV_{\text{QW}}}, \quad (6)$$

where I , q and V_{QW} are the operation current, the elementary charge and the QW volume, respectively. Therefore, the relation between the current density j and the carrier concentration n can be written as

$$j \cdot \text{CIE} = qd_{\text{QW}} (An + Bn^2 + Cn^3). \quad (7)$$

Multiplying (4) with (7), the carrier concentration n can be expressed by other parameters as:

$$n = \sqrt{\frac{j \cdot \text{EQE}}{Bqd_{\text{QW}}\text{LEE}}} \quad (8)$$

Inserting (8) into (7), we obtain the relation between j and $\sqrt{j \cdot \text{EQE}}$:

$$j = \frac{A}{\text{CIE}} \sqrt{\frac{qd_{\text{QW}}}{B \cdot \text{LEE}}} \sqrt{j \cdot \text{EQE}} + \frac{1}{\text{CIE} \cdot \text{LEE}} \left(\sqrt{j \cdot \text{EQE}} \right)^2 + \frac{C}{\text{CIE}} \sqrt{\frac{1}{qd_{\text{QW}}B^3\text{LEE}^3}} \left(\sqrt{j \cdot \text{EQE}} \right)^3. \quad (9)$$

j is a cubic polynomial function of $\sqrt{j \cdot \text{EQE}}$ with the constant term to be zero. By applying a polynomial fit to the curve of j versus $\sqrt{j \cdot \text{EQE}}$, one obtains the coefficients of all terms in (9). $\text{CIE} \cdot \text{LEE}$ is determined from the coefficient of the quadratic term

and the IQE is calculated as the ratio of EQE and CIE · LEE. A good estimation of LEE for a certain structure can be achieved by Monte Carlo ray tracing. It is reported to be about 23% for on-wafer measurements of a *c*-plane LED [9]. An enhanced LEE is expected for the two semipolar LEDs due to the 3D GaN surface morphology or the sapphire structurization. As a rough estimate, 40% of LEE is assumed in this study for both structures. Therefore, the CIE is acquired as the ratio of CIE · LEE and the assumed LEE.

The fitting principle of the PL data is similar as that of the EL data. The ratio of the integrated PL intensity I_{PL} and the power of the excitation source P_{PL} is proportional to the IQE:

$$\frac{I_{\text{PL}}}{P_{\text{PL}}} = \eta_1 \frac{Bn^2}{An + Bn^2 + Cn^3} \quad (10)$$

with η_1 denoting an unknown constant. The carrier generation rate G is proportional to the power of the excitation source:

$$G = \eta_2 P_{\text{PL}} \quad (11)$$

with η_2 denoting an other unknown constant. In steady state, the carrier generation rate is equal to the recombination rate, $G = R$. Considering (5), we get

$$\eta_2 P_{\text{PL}} = An + Bn^2 + Cn^3. \quad (12)$$

Putting (10) into (12), one can derive the relation between the parameters I_{PL} and P_{PL} as:

$$P_{\text{PL}} = A \sqrt{\frac{1}{B\eta_1\eta_2}} \sqrt{I_{\text{PL}}} + \frac{1}{\eta_1} \left(\sqrt{I_{\text{PL}}} \right)^2 + C \sqrt{\frac{\eta_2}{B^3\eta_1^3}} \left(\sqrt{I_{\text{PL}}} \right)^3 \quad (13)$$

P_{PL} is a cubic polynomial function of $\sqrt{I_{\text{PL}}}$ with the constant term to be zero. By applying again a polynomial fit to the curve of P_{PL} versus $\sqrt{I_{\text{PL}}}$, one obtains the value of $1/\eta_1$ as the coefficient of the quadratic term with which the absolute value of the IQE can be calculated according to (10).

4. Results

The *c*-plane LED, the stripe $\{10\bar{1}1\}$ LED and the planar $\{11\bar{2}2\}$ LED emit at 435 nm, 430 nm and 428 nm, respectively. As seen in Fig. 2, the *c*-plane LED has much higher output power in pulsed EL than the two semipolar ones. The fitting method is applied to all three structures to analyze whether the lower luminescence efficiency of the semipolar LEDs on foreign substrates is caused by lower CIE or lower IQE.

For the simple *c*-plane LED, a tight fit was obtained for the EQE curve (Fig. 3, left). CIE · LEE is determined to be 0.18 as the reverse value of the coefficient of the quadratic term in (9). Thus, the CIE is calculated to be 78% with the assumed LEE of 23% (Table 1). Similar IQE data versus current density have been measured on a sister wafer by T. Meyer in the characterization labs of Osram OS (Regensburg) [10] nicely confirming our

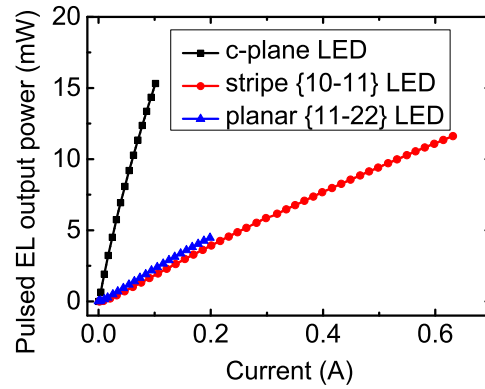


Fig. 2: The output power against the current of pulsed EL for c-plane LED, stripe $\{10\bar{1}1\}$ LED and planar $\{11\bar{2}2\}$ LED.

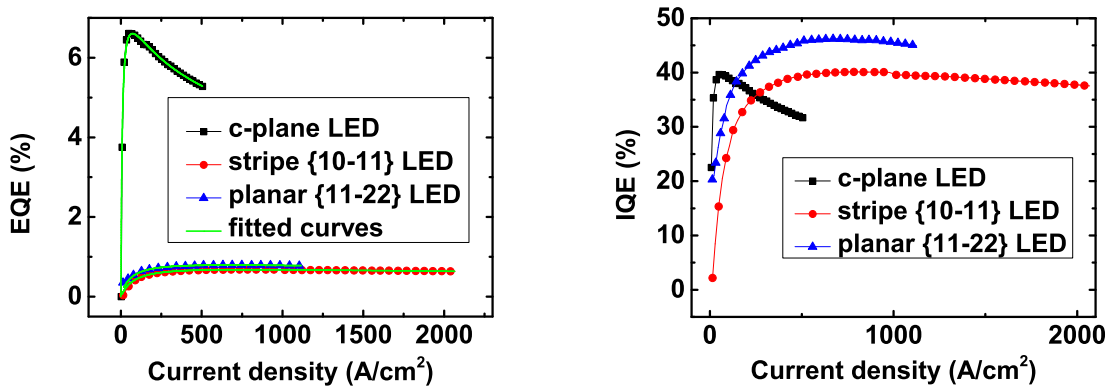


Fig. 3: EQE (left) and IQE (right) at different current density for the c-plane LED, the stripe $\{10\bar{1}1\}$ LED and the planar $\{11\bar{2}2\}$ LED.

evaluation method. From those results, we estimate a maximum error range of our IQE value of about 30 %.

Tight fits were obtained for the EQE curves of the two semipolar structures as well. CIE · LEE is determined to be 1.7 % and 1.7 % for the stripe $\{10\bar{1}1\}$ LED and the planar $\{11\bar{2}2\}$ LED, respectively. The corresponding CIE values are 4 % and 4 %, calculated with the assumed LEE values for the different structures (Table 1). Surprisingly, the CIE of the semipolar LEDs is much lower than 78 % of the c -plane LEDs! As seen in Fig. 3, both, the EQE and the IQE raise fast and start to decrease at a smaller current density for the c -plane LED as compared to the semipolar ones. The IQE of the semipolar LEDs is lower than that of the c -plane LED at low current density, but is similar and even higher at high current density. This can not explain the much higher EQE of the c -plane LED at all current densities. Obviously, the poor carrier injection is responsible for the not satisfying performance of the semipolar LEDs rather than the spectra and hence the crystal quality the InGaN/GaN QWs.

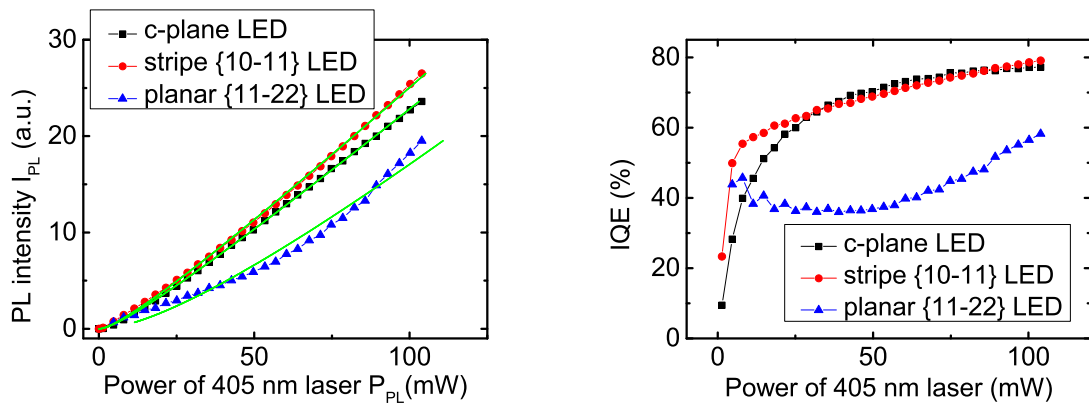


Fig. 4: The PL intensity I_{PL} dependent on the excitation power P_{PL} with the corresponding fitted curves (left) and the IQE estimated by the fit of the PL data (right) for the c -plane LED, the stripe $\{10\bar{1}1\}$ LED and the planar $\{11\bar{2}2\}$ LED.

For the PL measurements, the excitation power P_{PL} was varied from 1.4 mW to 104 mW by varying the driving current of the 405 nm laser diode. A stripe $\{10\bar{1}1\}$ structure with 5-fold InGaN/GaN QWs is employed in the PL measurement since the PL spectrum of the one with the single QW is so weak that it is covered by the spectral tail of the 405 nm laser diode. The quantum efficiency keeps increasing with increasing excitation power since the 405 nm laser diode does not have sufficient power to reach the high carrier concentration where the Auger recombination is expected to dominate. Therefore, the cubic term in (13) is skipped for the fit of the PL data. Reasonable fits were obtained for all three structures (Fig. 4, left). The lack of the data points over a sufficient large range of the carrier concentration would increase the error of the fitting. Nevertheless, the PL fit results in fairly the same IQE values for the c -plane and the stripe $\{10\bar{1}1\}$ LEDs and a slightly lower IQE value for the planar $\{11\bar{2}2\}$ LED (Fig. 4, right). The 35 % lower IQE of the planar $\{11\bar{2}2\}$ LED is definitely not the root reason for its inferior EL performance taking the big difference of the EL output power between the c -plane LED and the semipolar ones into account.

As indicated by the fits of the EL and PL data, the poor CIE rather than the IQE is the root reason for the low EQE of the semipolar LEDs. Therefore, it would be essential to improve the carrier transport or suppress the carrier leakage to achieve brighter semipolar LEDs. This may require to improve the electrical properties of the p-(Al)GaN layers, the p-doping profile or to optimize the AlGaN electron blocking layer and to eliminate any carrier tunneling channels, e.g., stacking faults intersecting the semipolar QWs [11].

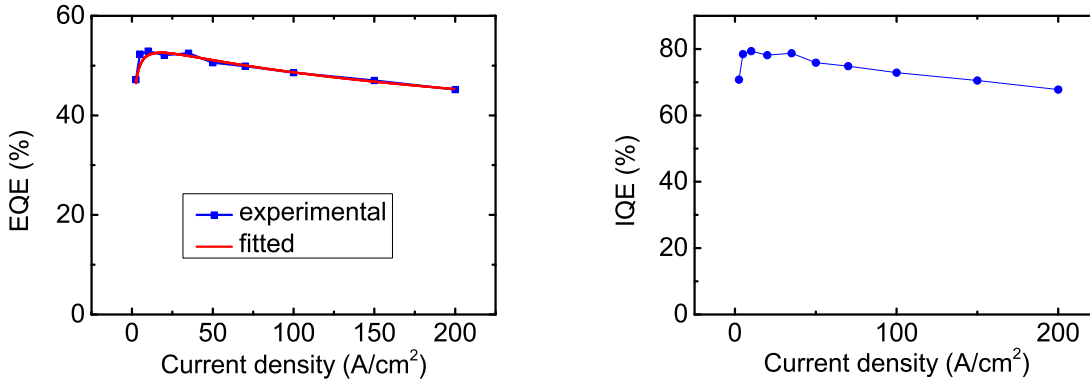


Fig. 5: The EQE curve according to the pulsed EL data and its fit (left) and the IQE curve determined by the fitting (right) dependent on the current density for the $\{20\bar{2}1\}$ LED on the native GaN substrate.

Is the low CIE an intrinsic problem of the semipolar GaN? To answer this question, we notice that UCSB reported a high-efficient semipolar $\{20\bar{2}1\}$ LED grown on native GaN substrates [12]. The ABC model is able to fit the pulsed EL data with a duty cycle of 1% very well (Fig. 5, left). $\text{CIE} \cdot \text{LEE}$ was determined to be 68% leading to $\text{CIE} > 68\%$. Hence, this LED does not suffer from the poor carrier injection. The estimated IQE reaches its maximum of $\sim 80\%$ at the current density of 10 A/cm^2 (Fig. 5, right). We see that the poor carrier injection limits the performance of the semipolar LED on the foreign substrate rather than that on the GaN native substrate.

The poor CIE rather than the IQE is the root reason for the low EQE of the semipolar LEDs on foreign substrates indicating that it would be essential to improve the carrier transport or suppress the electron spill-over to achieve brighter semipolar LEDs. Correspondingly, to improve the electrical property of p-(Al)GaN layers, p-doping profile or to optimize the AlGaN electron blocking layer could be good possibilities.

5. Summary

Pulsed EL measurements with a duty cycle of 1% were applied to c-plane, $\{10\bar{1}1\}$ and $\{11\bar{2}2\}$ LEDs to avoid diode heating. The fit of the pulsed EL data according to the ABC model allows us to obtain the IQE and CIE values. The IQE is comparable for all three structures whereas the CIE is determined to be 78% for the c-plane LED, but only about 4% for its semipolar counterparts. IQE values obtained by fitting resonant PL data confirm these findings. Hence, a poor charge carrier injection is responsible for

the lower efficiency of our semipolar LEDs grown on foreign substrates as compared to *c*-plane LEDs.

Acknowledgment

The authors gratefully acknowledge the discussion with Dario Schiavon (now with Top-GaN Lasers), the IQE measurement by Tobias Meyer (OSRAM), the technical support from M. Alimoradi-Jazi and R.F. Gul. This work has been financially supported by the German Federal Ministry of Education and Research (BMBF) in the project Hi-Q-LED (FKZ 13N9977).

References

- [1] K. Fujito, K. Kiyomi, T. Mochizuki, H. Oota, H. Namita, S. Nagao, and I. Fujimura, “High-quality nonpolar *m*-plane GaN substrates grown by HVPE”, *Phys. Status Solidi A*, vol. 5, pp. 1056–1059, 2008.
- [2] F. Scholz, “Semipolar GaN grown on foreign substrates: a review”, *Semicond. Sci. Technol.*, vol. 27, pp. 024002-1–15, 2012.
- [3] Q. Dai, M.F. Schubert, M.H. Kim, J.K. Kim, E.F. Schubert, D.D. Koleske, M.H. Crawford, S.R. Lee, A.J. Fischer, G. Thaler, and M.A. Banas, “Internal quantum efficiency and nonradiative recombination coefficient of GaInN/GaN multiple quantum wells with different dislocation densities”, *Appl. Phys. Lett.*, vol. 94, pp. 111109-1–3, 2009.
- [4] J. Hertkorn, F. Lipski, P. Brückner, T. Wunderer, S.B. Thapa, F. Scholz, A. Chuvilin, U. Kaiser, M. Beer, and J. Zweck, “Process optimization for the effective reduction of threading dislocations in MOVPE grown GaN using in situ deposited SiN_x masks”, *J. Cryst. Growth*, vol. 310, pp. 4867–4870, 2008.
- [5] T. Wunderer, P. Brückner, B. Neubert, F. Scholz, M. Feneberg, F. Lipski, M. Schirra, and K. Thonke, “Bright semipolar GaInN/GaN blue light emitting diode on side facets of selectively grown GaN stripes”, *Appl. Phys. Lett.*, vol. 89, pp. 041121-1–3, 2006.
- [6] F. Scholz, T. Meisch, M. Caliebe, S. Schörner, K. Thonke, L. Kirste, S. Bauer, S. Lazarev, and T. Baumbach, “Growth and doping of semipolar GaN grown on patterned sapphire substrates”, *J. Cryst. Growth*, vol. 405, pp. 97–101, 2014.
- [7] N. Okada, A. Kurisu, K. Murakami, and K. Tadatomo, “Growth of semipolar (11 $\bar{2}$ 2) GaN layer by controlling anisotropic growth rates in *r*-plane patterned sapphire substrate”, *Appl. Phys. Express*, vol. 2, pp. 091001-1–3, 2009.
- [8] N. Okada, K. Uchida, S. Miyoshi, and K. Tadatomo, “Green light-emitting diodes fabricated on semipolar (11 $\bar{2}$ 2) GaN on *r*-plane patterned sapphire substrate”, *Phys. Status Solidi A*, vol. 209, pp. 469–472, 2012.

- [9] T.X. Lee, K.F. Gao, W.T. Chien, and C.C. Sun, “Light extraction analysis of GaN-based light-emitting diodes with surface texture and/or patterned substrate”, *Optics Express*, vol. 15, pp. 6670–6676, 2007.
- [10] T. Meyer, OSRAM OS, *Private Communication*, Nov. 2014.
- [11] S. Faraji, “Epitaxy and characterization of semi-polar $(10\bar{1}1)$ and $(20\bar{2}1)$ GaN-based hetero-structures on $(11\bar{2}3)$ and $(22\bar{4}3)$ patterned sapphire substrate”, Master Thesis, Inst. of Optoelectronics, Ulm University, 2015.
- [12] Y. Zhao, S. Tanaka, C.C. Pan, K. Fujito, D. Feezell, J.S. Speck, S.P. DenBaars, and S. Nakamura, “High-power blue-violet semipolar $(20\bar{2}\bar{1})$ InGaN/GaN light-emitting diodes with low efficiency droop at 200 A/cm²”, *Appl. Phys. Express*, vol. 4, pp. 082104-1–3, 2011.